

# An algorithm for image stitching and blending

Vladan Rankov<sup>†</sup>, Rosalind J. Locke, Richard J. Edens, Paul R. Barber  
and Borivoj Vojnovic

Advanced Technology Development Group, Gray Cancer Institute, Mount Vernon Hospital,  
Northwood, Middlesex, HA6 2JR, United Kingdom;

## ABSTRACT

In many clinical studies, including those of cancer, it is highly desirable to acquire images of whole tumour sections whilst retaining a microscopic resolution. A usual approach to this is to create a composite image by appropriately overlapping individual images acquired at high magnification under a microscope. A mosaic of these images can be accurately formed by applying image registration, overlap removal and blending techniques. We describe an optimised, automated, fast and reliable method for both image joining and blending. These algorithms can be applied to most types of light microscopy imaging. Examples from histology, from *in vivo* vascular imaging and from fluorescence applications are shown, both in 2D and 3D. The algorithms are robust to the varying image overlap of a manually moved stage, though examples of composite images acquired both with manually-driven and computer-controlled stages are presented. The overlap-removal algorithm is based on the cross-correlation method; this is used to determine and select the best correlation point between any new image and the previous composite image. A complementary image blending algorithm, based on a gradient method, is used to eliminate sharp intensity changes at the image joins, thus gradually blending one image onto the adjacent 'composite'. The details of the algorithm to overcome both intensity discrepancies and geometric misalignments between the stitched images will be presented and illustrated with several examples.

**Keywords:** Image Stitching, Blending, Mosaic images

## 1. INTRODUCTION AND BACKGROUND

There are many applications which require high resolution images. In bright-field or epifluorescence microscopy [1], for example, which are used in biological and medical applications, it is often necessary to analyse a complete tissue section which has dimensions of several tens of millimetres, at high resolution. However, the high resolution single image cannot be realised with a low power objective, necessary to view a large sample, even if using cameras with tens of millions of active pixels. The most common approach is to acquire several images of parts of the tissue at high magnification and assemble them into a composite single image which preserves the high resolution. This process of assembling the composite image from a number of images, also known as 'tiling' or 'mosaicing' requires an algorithm for image stitching (registration) and blending. The automatic creation of large high resolution image mosaics is a growing research area involving computer vision and image processing. Mosaicing with blending can be defined as producing a single edgeless image by putting together a set of overlapped images [2]. Automating this process is an important issue as it is difficult and time consuming to achieve it manually. One such algorithm for image stitching and blending is presented in this paper.

Image stitching combines a number of images taken at high resolution into a composite image. The composite image must consist of images placed at the right position and the aim is to make the edges between images invisible. The quality of stitching is therefore expressed by measuring both the correspondence between adjacent stitched images that form the composite image and the visibility of the seam between the stitched images [3]. Image stitching (registration) methods have been explained in detail in [4]. In [5], cross-correlation is shown to be the preferred method for automatic registration of large number of images. Various registration methods were compared in this paper [5] and it was showed that the cross-correlation method provided the smallest error. When these methods were compared in terms of speed, the cross-correlation was shown to be the second fastest but much more accurate than the fastest method (principal axes method).

There are a number of papers that deal with the stitching problem [3, 6-8]. Image stitching can be performed using image pixels directly - correlation method; in frequency domain - fast Fourier transform method; using low level

---

<sup>†</sup>rankov@gci.ac.uk; phone +44 1923 828 611; fax +44 1923 835 210; www.gci.ac.uk

features such as edges and corners; using high level features such as parts of objects [2]. Brown [4] classifies image registration according to following criteria: type of feature space, type of search strategies and type of similarity measure.

Approaches for image stitching that optimise the search for the best correlation point by using Levenberg-Marquardt method are given in [2, 9, 10]. Levenberg-Marquardt method gives good results, but it is computationally expensive and can get stuck at local minima. An alternative way is to apply an algorithm which searches for the best correlation point by employing a 'coarse to fine' resolution approach in order to reduce the number of calculations [10, 11].

The approach offered in this paper makes the selection of the best correlation point in the following way. Based on knowledge about the expected overlap when using the motorised stage, it would be straightforward to find the best correlation point in the ideal case. However, the overlap area is not perfect, and certainly not to an accuracy of one pixel, due to deviations in stage position from the ideal and due to stage/camera misalignment. Our algorithm offers a way to overcome this problem by searching the small area around the expected central overlap pixel in order to find the best correlation point. Positioning of acquired images with a manual stage is much less accurate, so there is a need to search a wider area in order to find the best cross-correlation point.

Most of the existing methods of image stitching either produce a 'rough' stitch that cannot deal with common features such as blood vessels, comet cells and histology, or they require some user input [12]. The new algorithm presented in this paper has embedded code to deal with such features.

In order to remove the edges and make one compact image it is necessary to apply additional image blending. The process of image blending is restricted to zones of overlap which are determined during the stitching process. This means that if the overlap regions between images are large, and images are not perfectly matched on these parts, ghosting or 'blurring' is visible. However, if these regions are small, the seams will be visible [13]. In order to avoid these effects and make the blurring effect negligible, the cross-correlation function between the composite image and the image which is to be stitched needs to be applied appropriately. The new method presented in this paper shows that the best quality image can be achieved if blending is applied after each image has been stitched. This approach improves the stitching of additional images because the cross-correlation is applied to a blended composite image which gives a more robust result.

When acquiring images of highly non-uniform samples, as it is the case in our in vivo studies, the lighting conditions change and thus influence the cross-correlation applied during stitching. These lighting changes prevent the removal of artefacts. In order to avoid this effect it may be possible to normalise the illumination of the images, but it could cause some loss of information as one cannot be sure what the real cause for the variation in the image illumination is. It can come from the changes in the lighting but also from the different tissue colour. Hence, some illumination compensation is necessary.

Our achievement is a high-quality, automatic stitching and blending algorithm that responds to features such as blood vessels, comet cells and histology samples. The illumination compensation is not incorporated in the presented algorithm.

This paper is organised as follows. Section 2 explains the image acquisition process. Section 3 explains the methodology followed during the development of the image processing algorithm that applies both the stitching and blending. Section 4 gives the results of the applied algorithm on the selected images after the stitching only and after both stitching and blending and illustrates the effectiveness of the proposed algorithm. Conclusions are presented in Section 5 and directions for the future work are defined.

## 2. IMAGE ACQUISITION

### 2D images

All images were acquired using a standard microscope. All 2D images were acquired by sample translation and collected either manually or automatically using the motorised stage. Three types of 2D images were acquired. These include the images of histology, fluorescent cells as part of a comet array (comet cells) and in vivo blood vessels. The setup specification for these images is summarised in Table 1. CCD cameras were used to acquire the images with either a IEEE 1394 interface or using a PCI frame grabber (type: by National Instruments, UK). The imaging area is of the order of  $1 \times 1 \text{ mm}^2$  when using objective x10. CCD cameras introduce two noise effects. One is a dark current and another is a non-uniform pixel response. In order to cancel out the dark current effect, images acquired with no light were subtracted from images of the sample. For cancellation of the non-uniform pixel response, the image of the sample is divided by a blank image acquired with standard illumination of a clean slide. Lens aberrations are also present. All imaging systems, due to such aberrations, suffer to a greater or lesser extent from barrel or pincushion distortion, or their combination. The most difficult conditions for image stitching are those with wide range of ambient lighting i.e.

with a large intensity span - spatially varying illumination. It is assumed that rotation and scaling stay the same throughout both the experiments and processing the images. Only translation errors need to be corrected during the stitching process.

	<b>Histology</b>	<b>Comet cells</b>	<b>Blood vessels</b>
<b>Stage</b>	Motorised stage with a positioning accuracy $\pm 1\mu\text{m}$ .		Manual stage
<b>Microscope</b>	Nikon TE 2000	Nikon TE 200	Nikon Diaphot 200
<b>Camera</b>	Colour JVC KY-F75U 3CCD camera used mostly for bright field histology and Hamamatsu Orca Monochrome for fluorescence histology	Monochrome Hamamatsu Orca cooled CCD camera	Colour camera JVC KY-55 3CCD
<b>Computer Interface</b>	All images were digitised and captured in the memory of a PC using IEEE1394		All images were digitised and captured with NI1408 frame grabber
<b>Objectives</b>	Objectives are from x4 to x60, but in most cases x10 with a resolution in the region of $0.85\mu\text{m}/\text{pixel}$ . If stitching of the images is necessary, then x4 objective is mostly used.		
<b>Resolution</b>	1344x1024 pixels	1344x1024 pixels	758x576 pixels

Table 1 Summary of the setup specification used for the image acquisition

### 3D images

For the acquisition of 3D images the following setup was used. A Nikon TE 200 fluorescence microscope was used with a modified stage to accommodate rodents. Our *in vivo* blood vessel images were acquired through a window chamber arrangement. It consists of double sided aluminium frame holding two parallel glass windows. It is located centrally above the objectives [14]. Tumour angiogenesis and vascular response to treatment in both the morphology of blood vessel networks and the function of individual vessels have been investigated using the window chamber. Multi-photon microscopy techniques have been applied to obtain 3D images of tumour vasculature [15], as these techniques are shown to be highly effective in obtaining three-dimensional biological images.

The multi-photon microscope system is based on Bio-Rad MRC 1024MP workstation and consists of a solid-state-pumped (10W Millennia X, Nd:YVO<sub>4</sub>, Spectra-Physics), self-mode-locked Ti:Sapphire (Tsunami, Spectra-Physics) laser system, a focal scan-head, confocal detectors and an inverted microscope (Nikon TE200) [15].

Multi-photon microscopy can accurately locate fluorescence within a 3D volume and can be successfully applied to the analysis of vascular morphology.

Usually a small tumour (few millimetres in diameter) was implanted into the skin in the window chamber. The whole tumour vasculature was imaged for most experiments. Images were taken with 10X objective for all but the smallest tumours and image covered approximately 1.3x1.3 mm tissue. Stacks of images are taken with a typical stack of 50 slices. It takes typically 13 minutes to acquire images for an entire stack.

## 3. IMAGE PROCESSING - METHODOLOGY

There are two main stages in processing these images:

1) Image stitching

Stitching is performed by sliding the new image over the composite image and finding the best cross-correlation point.

2) Image blending

Blending was done by separating colour planes, where necessary, applying blending algorithm for each colour band and recomposing planes together to get full colour image at the output. The blended images should maintain the quality of the input images [16].

These processes are explained in detail below and refer to 2D images unless specified that they refer to 3D images.

Algorithms were developed in C programming language under LabWindows/CVI 7.0 (National Instruments) development environment, using IMAQ Image Processing Library and Windows XP Professional operating system. The algorithms are completely automated and they have been tested on a PC with processor speed 1.53GHz and 448MB of RAM.

### 3.1 Stitching method

In the presented algorithm the stitching is performed by image translation only. The applied procedure can be referred to as mosaicing, tiling, montaging or stitching. The first step is the generation of relative positions of acquired images and the creation of an empty image array in computer memory where these images will be placed. The next step is a search for the point of best correlation which is performed by sliding adjacent image edges in both directions until the best match of edge features is found. This search process requires the choice of an optimum search space shown in Figure 1, in which a search is performed for the best correlation. The use of too many pixels inside this box makes the correlation process time consuming whilst too few pixels reduce the quality of match. The choice of number of pixels used is strongly related to the dimensions of features expected to be visible in the image which in turn depends on focus quality, i.e. on the maximum spatial frequencies present in the image.

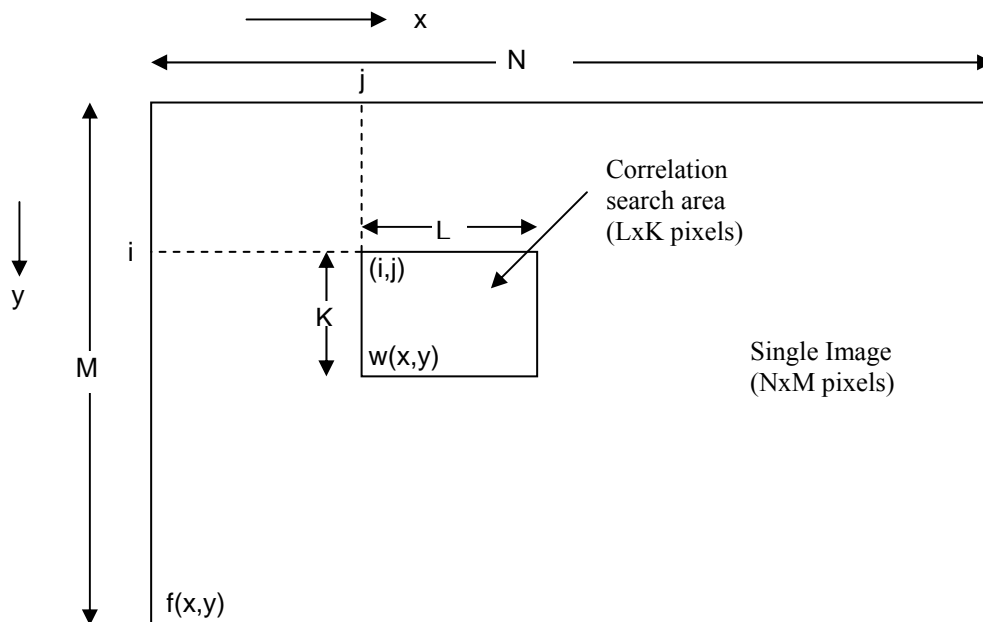


Figure 1: The general normalised cross correlation procedure is performed within a small search area.

The normalised cross correlation coefficient for the case above is defined as in equation (1):

$$\text{cross-correlation} = \frac{\sum_{x=0}^{L-1} \sum_{y=0}^{K-1} (w(x, y) - \bar{w})(f(x + i, y + j) - \bar{f}(i, j))}{\sqrt{\sum_{x=0}^{L-1} \sum_{y=0}^{K-1} (w(x, y) - \bar{w})^2} \sqrt{\sum_{x=0}^{L-1} \sum_{y=0}^{K-1} (f(x + i, y + j) - \bar{f}(i, j))^2}} \quad (1)$$

Where  $w(x, y)$  represents a pixel value of the image to be placed;  $\bar{w}$  is the mean value of all pixels included in the box area;  $f(x+i, y+j)$  represents a pixel value of the composite image inside the box area;  $\bar{f}(i, j)$  is the mean value of all pixels of the composite image within the box area and parameters  $K, L$  represent the box dimensions in number of pixels included.

In the case where images of equal dimensions are to be stitched it is usually sufficient to extract a narrow strip from the edge of one image and to correlate this with a larger rectangle from the other. If there are features having reasonable contrast, the strip can be as small as 3 pixels wide to obtain an unambiguous point of best correlation. This approach gives rise to a lengthy and CPU-intensive series of calculations. However, there are ways in which the process can be optimised. Recalculation of part of equation (1) (equation (2)) is not necessary for every point as pixel values of the overlapping image inside the bounded box stay the same during the correlation search.

$$Cn1 = \sqrt{\sum_{x=0}^{L-1} \sum_{y=0}^{K-1} (w(x, y) - \bar{w})^2} \quad (2)$$

Additionally, if features are large enough, the sub-sampling of images may be performed to reduce the total number of pixels in order to get information about approximate location of the best correlation point. This information can then be used for a finer search at full resolution over a small area around this point.

When images are acquired using a motorised stage the overlap between images is known and hence it is only necessary to search a small region. For the motorised stage, the overlap area mainly covers 10% of the image and the box area used is 40x40 pixels. If the overlap is not known as is the case when using the manual stage, the correlation function searches area of 350x350 pixels.

It is possible to correlate the edges of images in the same order as they were acquired, but it may not be the most efficient approach. Acquisition is most readily performed in a snake-like raster scan pattern. When applying the correlation function, however, it is better, although less convenient, to follow a spiral-like pattern, from the centre outwards. The justification for such an approach is as follows: Histology sections tend to be round and therefore, the only information available for correlation at the corners of the area scanned is due to dirt on the slide. By starting in the middle, greater weight is given to the area containing information of interest. This method is also applicable to sets of images that are acquired manually (without the use of motorised stage) and overlaps are unknown and uneven in this case images at the corners of the rectangular region may not even have been acquired.

It may often be the case, especially when working with weakly fluorescing samples, that a good point of correlation cannot be found. Correlation gives value from 0 to 1 where 1 is the perfect correlation. If coefficient is greater than 0.7 it represents a 'good' cross-correlation. This value is established empirically. In a case when the correlation higher than 0.7 cannot be found, a 'hole' is left in the composite mosaic image. When all possible images have been placed, it is likely that there will be more information available for correlation, e.g. the 'hole' may be surrounded with images on all four sides which can then be used to find a best match. A second pass of the spiral will generally fill all such holes successfully. At the corners of the region there may be no information at all if the slide was very clean and we are dealing with a circular or convex sample. In this case there is little choice but to assume the position of the images based on the known stage position at the time of acquisition. In any case, such featureless regions will probably be of little interest or importance.

When stitching the histology images taken with a colour camera, only the intensity component has been used for the search for best correlation. In case of blood vessels, colour images give better results, if contributions of basic colours are in the ratio red – 26%, green - 50% and blue component – 24% as this improves vessel/tissue contrast. Different frequency bands contribute with different proportion. It proved unnecessary to segment the blood vessels and correlate according to the edges. When processing images of comet cells which are 16-bit monochrome images, due to sparse data, there may not be any information available in the overlap region. A threshold method is used to find bright objects (comet cells), if any, in the overlap region, and then the centre of the layout is used to determine a 40x40 rectangular region which is searched for the point of best correlation.

For processing the vasculature images the following procedure can be used: The software calculated image processing functions to find visible vessels and make vessel skeleton map. Ridge filters were used to enhance the vessel structure. A binary image was obtained using thresholding and skeletonisation and a vessel map was calculated to form 1-pixel-

width lines. This method was compared with ordinary cross-correlation method and since it did not yield better result, intensity cross-correlation was used [15].

The three-dimensional stitching method firstly selects one of the images from the first stack. Then, the corresponding image is selected from the neighbouring stack. The best relative position for these two images is found using normalised cross-correlation explained earlier. When the best position is found, whole stacks were positioned according to the position found from these two images. The seams were removed using mean pixel blending for overlapped regions [17]. A search region of approximately 50% of the image gave best results because the adjacent images may have different brightness levels. The large overlap smoothes out the intensity variation [6].

### 3.2 Gradient blending method

In most cases neighbouring image edges show intensity discrepancies which are undesirable. These variations in intensity are present even when cross-correlation is almost perfect to the eye. In order to eliminate such effects, a blending or ‘feathering’ algorithm is applied.

Using the blending method, which applies changes in intensity, makes quantitative analysis of intensities invalid. The advantage of using blending method is in improving visual quality of the composite image and making the edges invisible.

The composite image consists of a number of images that are initially placed next to each other. In a case of manually taken images, images are placed using visual inspection, whilst in a case of motorised stage, relative positions are known. An empty composite image of adequate size is firstly created. Images are then placed in a spiral-like pattern described previously, starting with central image.

Each image in turn is put in the composite image and its position is determined by cross-correlation between the new image and the composite image. The blending algorithm is then applied and the process is repeated for all other images. In figure 2 the overlap between a new image and the composite image is shown (gray area). In the overlapped area the image blending algorithm calculates the contribution of the new image and the composite image at every pixel. A look up table is created for each new image and it has the size and shape of the overlap. This look up table is normalised in order to define what proportion of intensities of two overlapped regions is used for generating the new composite image. One value of the normalised look up table can be perceived as a weighting factor at every pixel. The right image of figure 2 represents a mask, which is created for each overlapped image of the weighting ( $\alpha$ ) which is calculated as a distance from the image edge. The blended image consists of pixels:

$$N(x, y) = \alpha I(x, y) + (1 - \alpha)C(x, y) \quad (3)$$

where,  $C(x, y)$  is the composite image pixel (before placing the new image),  $I(x, y)$  is the new image pixel and  $N(x, y)$  the new composite image pixel (with new image added).

The blending algorithm minimises effects of intensity variations, removes the edges and improves the cross-correlation.

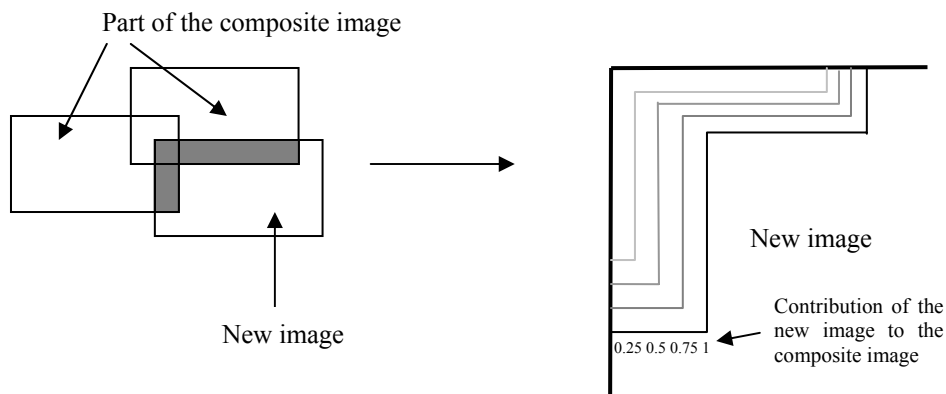


Figure 2: Procedure for blending intensities of overlapping images

This approach has been applied onto three types of images: RGB images, I16 (16 bit images) and 8bit grayscale images. RGB images were firstly decomposed into three-band planes, the blending algorithm was then applied to each band and finally image planes were recombined again.

#### 4. RESULTS

##### 2D Images

The methods described above were evaluated on real histology, blood vessel and comet cells images. Figures 3, 4 and 5 show results for in vivo blood vessel images taken with a manual stage. Figure 3 represents the composite image created by positioning the images one next to each other as they were acquired. Figure 4 shows the image resulting after applying the cross-correlation procedure for image stitching.

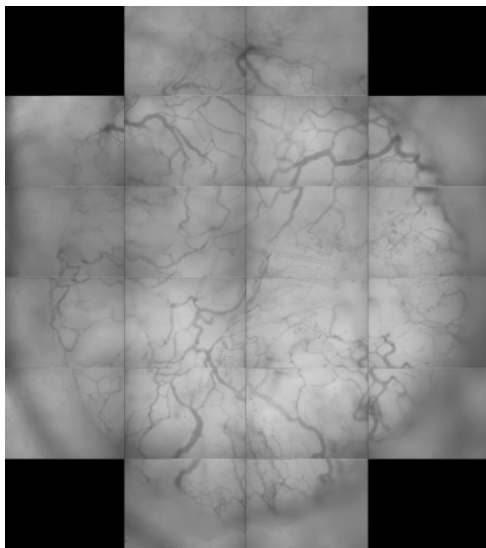


Figure 3: Unprocessed composite image

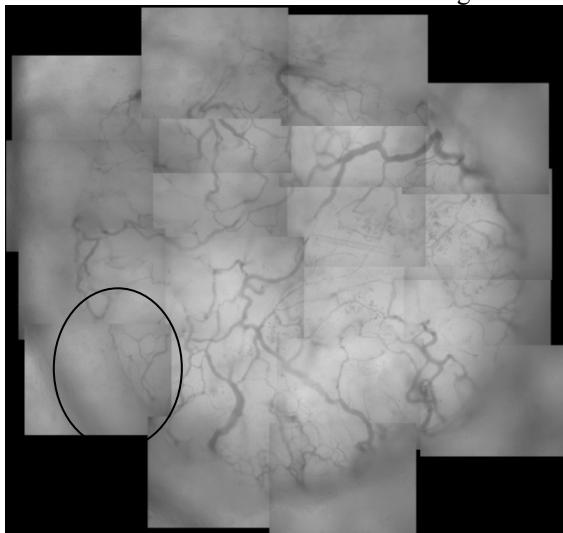


Figure 4: Images sorted using cross-correlation

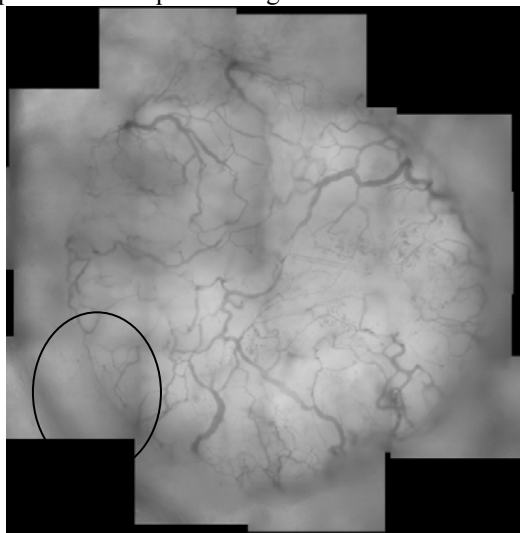


Figure 5: Resulting image after cross-correlation and blending

It can be seen that the correct position of images are mostly found, but seams are still visible and therefore the information from the image is reduced. These seams are removed by applying the gradient blending method which is shown in Figure 5.

The blending algorithm is fast and for the presented images (Figures 3-5) of blood vessels it took 71.2 seconds for the stitching of 24 1.3MB images, whilst for both stitching and blending it takes 79.2 seconds.

The best stitching precision achieved is 1 pixel for the x10 magnification whilst the resolution is 0.85 microns/pixel.

The marked areas in Figures 4 and 5 show how the correlation between images has been improved with the application of blending algorithm. As a result, the edges are eliminated, so the next image has better chance to be placed to the right position.

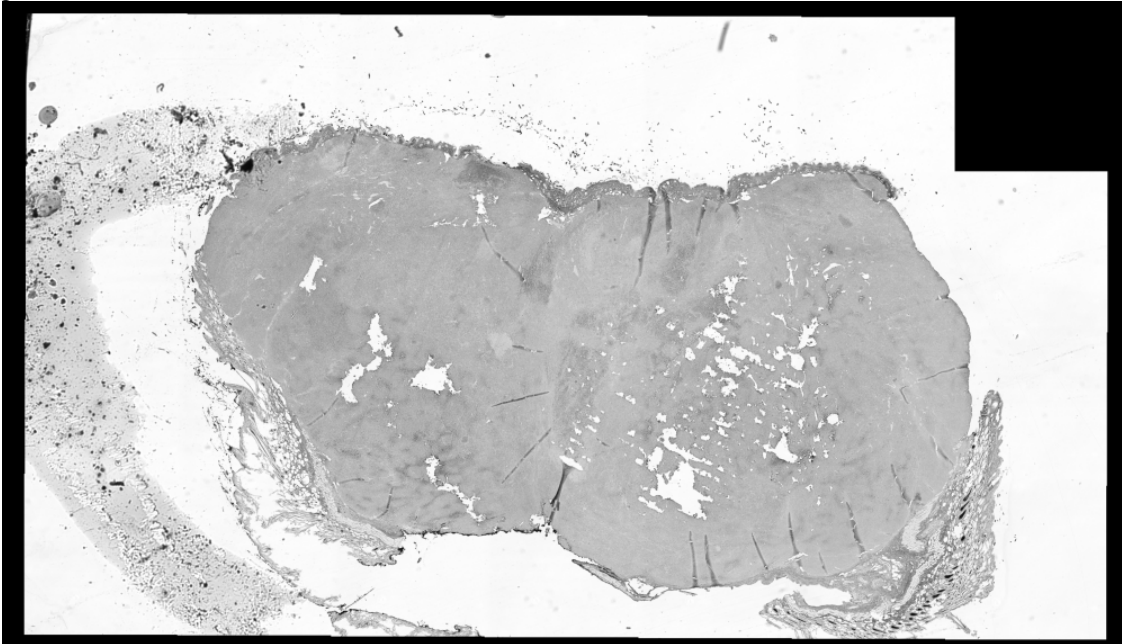


Figure 6: Blended histology –image acquired using motorised stage

Figure 6 represents 28 3MByte colour RGB images stitched together. Images are taken with a magnification x4 and the size of the sample is 2mmx2mm per image. Each image has dimension of 1024x1024 pixels. The composite image that represents the histology has dimensions 14mmx8mm. Time necessary to implement stitching is 21.41 seconds and time required to do both stitching and blending is 39.4 seconds. Image at the top right corner could not be stitched because there was not enough information (features) to determine the right position.

### 3D Images

Figure 7 represents the tumour of the order of 1mm in diameter. The presented composite image consists of 3x2 sets of images. The input image set has 80Mbytes and the output image set after correlation and blending has 65Mbytes. Each of six 13 Mbytes stacks consists of 51 image planes with each image having 512x512 pixels. It takes 31.5 seconds to correlate and blend all images.

The process of correlation and blending the images can be explained in the following way. The first step is to select the set of six best images, one from each of the six stacks, to use it for correlation. Ideally, the image chosen from the stack needs to have both the best contrast and the highest number of features. One image is taken from the stack and correlated with the corresponding image from the other stack. They are expected to come from the same plane, although this is not necessarily the case as with use of a manual stage it was not possible to precisely replicate the z position for each stack. This process of selecting the initial set of images has been done empirically. The middle image is usually selected from the stack as the best candidate for correlation. All correlation points are then found between the selected (usually middle) images and the images from other planes are stitched and blended correspondingly. The average blending has been applied on all images.

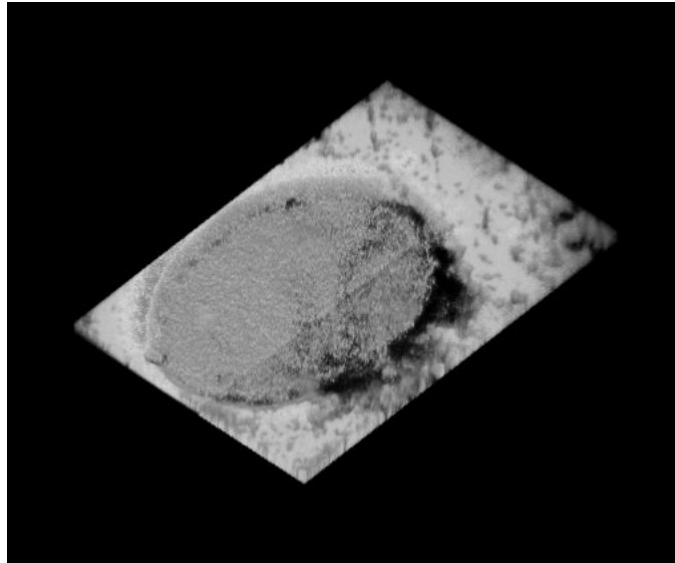


Figure 7: Stitched 3D image of tumour in a window chamber

## 5. DISCUSSION AND FUTURE WORK

### 2D Images

A new approach for generating edgeless blended, high resolution, composite image using cross-correlation and blending has been presented. In order to correctly register the image onto composite image, the cross-correlation method has been used. Regions of overlap were calculated. One image at a time is correlated with composite image and when image is registered the blending is performed.

The presented method is fast, effective and gives considerable improvements in visual effects of the stitched images compared to the existing methods. Blending method is particularly fast because it uses a Look Up Table technique. Blending also improves the normalised cross-correlation (see Figures 4. and 5.)

Future work will include an algorithm for both the illumination compensation and reduction of the blurriness.

### 3D Images

3D correlation has been done, as well as the basic 3D blending. The next step is to implement a gradient blending for 3D images. Due to movement of the imaged sample during acquisition, the mismatch in the z plane is present and hence the corresponding planes need to be found. Automation of the whole process will also form the part of the future work.

## ACKNOWLEDGMENTS

We would like to thank Professor Gillian M. Tozer, Mr. Ian Wilson and Dr. Vivien E. Prise of Tumour Microcirculation Group at Gray Cancer Institute and Dr. Dawn Carnell of Paul Strickland Scanner Centre at Mount Vernon Hospital for acquiring and providing us with their images.

We also would like to acknowledge Cancer Research UK for financial assistance through programme grant C133/A1812. We gratefully acknowledge financial support of the UK Research Council's Basic Technology programme as well.

## REFERENCES

1. White, N., Errington, R., *Fluorescence techniques for drug delivery research: theory and practice*. Advanced Drug Delivery Reviews, 2005. 57: p. 17-42.
2. Bhosle, U., Chaudhuri, S., and Roy, S., *A Fast Method for Image Mosaicing using Geometric Hashing*. IETE Journal of Research, 2002. 48(3&4): p. 317-324.

3. Levin, A., Zomet, A., Peleg, S., and Weiss, Y., *Seamless image stitching in the gradient domain*. 2003, Hebrew university.
4. Brown, L.G., *A survey of image registration techniques*. ACM Computing Surveys, 1992. 24: p. 325-376.
5. Flynn, A., Green, A., Boxer, G., Pedley, R., and Begent, R., *A comparison of image registration techniques for the correlation of radiolabeled antibody distribution with tumor morphology*. Phys. Med. Biol., 1999. 44: p. N151-N159.
6. Chen, S., *QuickTime VR - An Image-Based Approach to Virtual Environment Navigation*, in *Apple Computer Inc.* 1995.
7. Kanazawaa, Y., Kanatani, K., *Image mosaicing by stratified matching*. Image and Vision Computing, 2004. 22: p. 93-103.
8. Debevec, P., Yu, Y., and Borshukov, G., *Efficient View-Dependent Image-Based Rendering with Projective Texture-Mapping*. 2001.
9. Szeliski, R., *Video Mosaics for Virtual Environments*. IEEE Computer Graphics and Applications, 1996. 16(2): p. 22-30.
10. Hsieh, J.-W. *Fast stitching algorithm for moving object detection and mosaic construction*. in *IEEE International Conference on Multimedia & Expo*. 2003. Baltimore, Maryland, USA.
11. Chalermwat, P.a.E.-G., *Multi-resolution Image Registration Using Genetics*. 1999.
12. Uyttendaele, M., Eden, A., Szeliski, R., *Eliminating Ghosting and Exposure Artefacts in Image Mosaics*. CVPR, 2001. II: p. 509-516.
13. Baumberg, A. *Blending images for texturing 3D models*. in *BMVC*. 2002.
14. Tozer, G., Prise, V., Wilson, J., Cemazar, M., Shan, S., Dewhurst, M., Barber, P., Vojnovic, B., and Chaplin, D., *Mechanisms Associated with Tumour Vascular Shut-Down Induced by Combretastatin A-4 Phosphate: Intravital Microscopy and Measurement of Vascular Permeability*. Cancer Research, 2001. 61: p. 6413-6422.
15. Tozer, G., Ameer-Beg, S., Baker, J., Barber, P., Hill, S., Hodgkiss, R., Locke, R., Prise, V., Wilson, I., Vojnovic, B., *Intravital imaging of tumour vascular networks using multi-photon fluorescence microscopy*. Advanced Drug Delivery Reviews, 2005. 57: p. 135-152.
16. Chen, C., Klette, R., *Image stitching - Comparisons and New Techniques*. Computer Analysis of Images and Patterns, 1999. 1689: p. 615-622.
17. Ameer-Beg, S., Edme, N., Peter, M., Barber, P., Vojnovic, B., *Imaging Protein-Protein Interactions by Multiphoton FLIM*. SPIE-OSA Biomedical Optics, 2003. 5139: p. 180-189.